Role of Dibromomalonic Acid in the Photosensitivity of the $Ru(bpy)_3^{2+}$-Catalyzed Belousov−Zhabotinsky Reaction

Vladimir K. Vanag,* Anatol M. Zhabotinsky, and Irving R. Epstein

Department of Chemistry and Volen Center for Complex Systems, MS 015, Brandeis University, Waltham, Massachusetts 02454-9110

Received: April 14, 2000; In Final Form: June 29, 2000

Dibromomalonic acid (Br_2MA) oxidizes the photoexcited state of the $Ru(bpy)_3^{2+}$ complex, producing Br_2. Br_2MA also reduces $Ru(bpy)_3^{3+}$, yielding Br^-. The first of these reactions has a rate proportional to $[H^+]$ and plays an important part in the mechanism of photoinhibition of the Belousov−Zhabotinsky reaction. We propose a reaction mechanism that gives good agreement with the experimental data.

I. Introduction

The photosensitive Belousov−Zhabotinsky (BZ) reaction catalyzed by the $Ru(bpy)_3^{2+}$ metallo-complex has been widely utilized in recent years. It has been employed in image processing,[1] for pattern formation,[2] in studying traveling,[3] spiral,[4,5] and scroll waves,[6] as well as in investigations of stochastic resonance.[7−9] Understanding the mechanism of photosensitivity in this reaction may facilitate the use of light as a precise tool for external quantitative control of the BZ reaction.

A number of authors have discussed the mechanism of light sensitivity in this reaction.[10−15] For the inorganic part of the BZ reaction (i.e., without malonic acid (MA)), the main effect of light is the production of $BrO_2^\bullet$ via (R1)−(R3),[10]

$$\mathrm{Ru(II)} + h\nu \rightarrow \mathrm{Ru(II)^*} \qquad v(I_0) \qquad \text{(R1)}$$

$$\mathrm{Ru(II)^*} \rightarrow \mathrm{Ru(II)} \qquad k_2 \qquad \text{(R2)}$$

$$\mathrm{Ru(II)^* + BrO_3^- + 2H^+ \rightarrow Ru(III) + BrO_2^\bullet + H_2O} \qquad \text{(R3)}$$

which are followed by the autocatalytic cycle:

$$\mathrm{Ru(II) + BrO_2^\bullet + H^+ \rightarrow Ru(III) + HBrO_2} \qquad \text{(R4)}$$

$$\mathrm{BrO_3^- + HBrO_2 + H^+ \rightarrow 2BrO_2^\bullet + H_2O} \qquad \text{(R5)}$$

where Ru(II) and Ru(II)* are $Ru(bpy)_3^{2+}$ and its photoexcited-state $Ru(bpy)_3^{2+}$*, respectively, Ru(III) is $Ru(bpy)_3^{3+}$, $v(I_0)$ is the rate of Ru(II)* photogeneration in reaction (R1), which depends on the light intensity I_0, and k_2 is the total first-order rate constant for all deactivation processes, including Ru(II)*-quenching by O_2 when this species is present.

For the full BZ system with MA, and consequently in the presence of a relatively high concentration of bromomalonic acid (BrMA), the main route of photoresponse of the BZ reaction involves production of bromide[15,16] through reactions R1, R2, and R6, R7,

$$\mathrm{Ru(II)^* + BrMA \rightarrow Ru(III) + MA^\bullet + Br^-} \qquad k_6 \qquad \text{(R6)}$$

$$\mathrm{Ru(III) + BrMA \rightarrow Ru(II) + BrMA^\bullet + H^+} \qquad k_7 \qquad \text{(R7)}$$

where $BrMA^\bullet$ and $MA^\bullet$ are bromomalonyl radical, $^\bullet CBr(COOH)_2$, and malonyl radical, $^\bullet CH(COOH)_2$, respectively. Kádár et al.[16] showed experimentally that, if the concentration of Ru(II) is high enough (all actinic light in the range 400−500 nm is absorbed by the reaction mixture), then the rate of bromide photoproduction in the organic subsystem of the BZ reaction (BrMA, Ru(II), and H_2SO_4) under anaerobic conditions (constant flow of argon gas) may be expressed as

$$\frac{\mathrm{d[Br^-]}}{\mathrm{d}t} = \frac{2v(I_0)k_6[\mathrm{BrMA}]}{k_2 + k_6[\mathrm{BrMA}]} \qquad (1)$$

where $k_2/k_6 = 8.9 \times 10^{-2}$ M and the factor of 2 in the numerator arises from the fact that there are typically two ions of Br^- produced for each Ru(II)* in reactions R6 and R7, because $BrMA^\bullet$ releases an additional bromide ion in subsequent reactions.

Equation 1 is useful, but it may be incomplete for the full BZ reaction. Apart from BrMA, other bromoderivatives of malonic acid arise in the full BZ reaction. The most important of these is dibromomalonic acid (Br_2MA), which is formed in the following reaction.

$$\mathrm{Br_2 + CHBr(COOH)_2 \rightarrow CBr_2(COOH)_2 + H^+ + Br^-} \qquad \text{(R8)}$$

According to Försterling,[17,18] the concentration of Br_2MA can be quite high if the sum of the initial bromide and bromate concentrations is comparable with [MA]. This situation occurs in many pattern formation experiments.[1,2,19] It seems reasonable to assume that a reductant as strong as Ru(II)* can be oxidized by Br_2MA in reaction R9,

$$\mathrm{Ru(II)^* + Br_2MA \rightarrow Ru(III) + products} \qquad k_9 \qquad \text{(R9)}$$

producing either Br_2 or Br^-. Reaction R9 may make a significant contribution to the total bromide photoproduction rate. We examine this hypothesis below.

II. Experimental Section

A schematic drawing of the experimental configuration is shown in Figure 1. The analyzing light from a 45 W tungsten lamp (L1) passes through a set of lenses, an interference filter (IF) with maximum at $\lambda_{max} = 620$ nm, and a reactor. The beam is then directed to a photomultiplier (PM) in front of which a

10.1021/jp001418m CCC: $19.00
Published on Web 08/11/2000

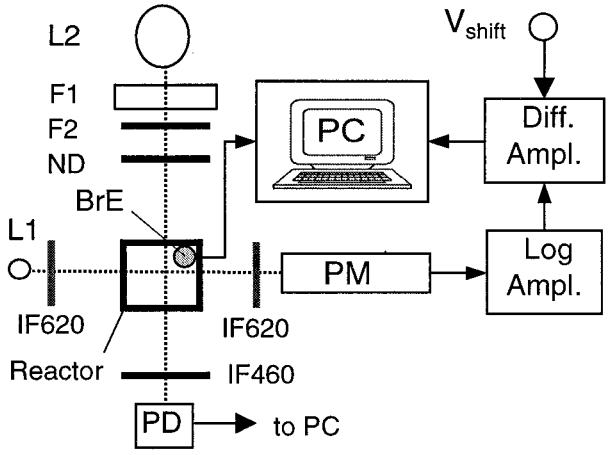

Figure 1. Experimental setup. See text for details.

second IF with the same λ_{max} is placed. The wavelength 620 nm corresponds to the absorption band of $Ru(bpy)_3^{3+}$. The signal from the PM is passed through a logarithmic amplifier, which allows us to measure directly the changes in absorption. The signal then goes to a differential amplifier, which enables us process the signal before its acquisition by a personal computer (PC). We use a 20 mL thermostated Teflon reactor, which has four flat quartz windows.[20] All experiments are run at $t = 25$ °C. A bromide-selective electrode (BrE) (Orion) is inserted into the stopper of the reactor in such a way that no light illuminates the electrode membrane. A silver chloride reference electrode is connected with the reactor through a Na_2SO_4 salt bridge. As a source of actinic light, we use a 150 W xenon arc lamp (L2) (Oriel), the light of which passes through a heat (water) filter (F1), a 400−500 nm band-pass blue filter (F2) (Oriel), and neutral density filters (ND). The light intensity is measured with a power meter (Newport, model 1815-C). During illumination of the reaction mixture, the power meter with an IF at $\lambda_{max} =$ 460 nm placed in front of its photodiode (PD) is used as another photodetector to measure the absorption of $Ru(bpy)_3^{2+}$. The signals from BrE, PM, and PD are collected by the personal computer.

Commercially available analytical grade reagents (sodium bromide, sodium bromate, malonic acid, H_2SO_4, $Ru(bpy)_3Cl_2$, and cerium(IV) sulfate tetrahydrate) were used without further purification.

Malonic acid was brominated completely in a mixture of MA, BrO_3^-, Br^-, and H_2SO_4 with initial concentrations of malonic acid, bromate, and bromide corresponding to the stoichiometry of the overall reaction R10.

$$3MA + 2BrO_3^- + 4Br^- + 6H^+ \rightarrow 3Br_2MA + 6H_2O \qquad \text{(R10)}$$

Under these conditions, the reaction scheme of Sirimungkala et al.[18] presented in Appendix 1 implies that very little BrO_3^-, Br^-, MA, and BrMA should remain in solution after bromination.

Experiments with the $Br_2MA-Ru(III)$ subsystem were run as follows. First, MA, BrO_3^-, Br^-, and H_2SO_4 were mixed in the ratio $[MA]_0:[BrO_3^-]_0:[Br^-]_0 = 3:2:4$. In most sets of experiments, the initial $[H_2SO_4]$ was chosen so that after bromination $[H^+] = 0.5$ M at each set of initial concentrations of the other reagents. In another set of experiments, the final value of $[H^+]$, 0.25, was then increased to the desired value by addition of sulfuric acid. In calculating $[H^+]$ we took $\Delta[H^+] = 3[Br^-]_0/2 = 3[BrO_3^-]_0$ and K_{a2} for H_2SO_4 as 0.012. We checked the desired reactant ratios by titration while simultaneously recording the absorbance at the peak of the Br_2 spectrum, 400 nm, Abs_{400}. The small amount of Br_2 produced gives an absorbance that is recorded with an accuracy $\Delta Abs/(l\epsilon_{400}) = 2 \times 10^{-6}$ M, where $\Delta Abs = 0.001$ is the resolution of our spectrometer, $l = 3$ cm (optical path length of the reactor), and $\epsilon_{400} = 170\ M^{-1}\ cm^{-1}$ is the extinction coefficient of Br_2 at this wavelength.[18] If $[MA]_0 \le 3[Br^-]_0/4 = 3[BrO_3^-]_0/2$, Abs_{400} shows a smooth, exponential decrease to its final value that exceeds the absorbance of the reactor filled with pure water, Abs_0, by $[Br_2]l\epsilon_{400}$. If $[MA]_0 > 3[BrO_3^-]_0/2$, the curve of decreasing $Abs_{400}(t)$ meets the final horizontal line Abs_{final} at a sharp angle, in this case $Abs_{final} = Abs_0$. The kinetic curves for Br_2 (absorption at $\lambda = 400$ nm) and Br^- (bromide-selective electrode) are in good agreement with the corresponding simulated curves obtained using the reaction scheme in Appendix 1. To an accuracy of better than 10^{-5} M, our measurements show that after complete bromination in accord with reaction R10 no MA or BrO_3^- are left in the reactor.

Thirty minutes after the beginning of the bromination, when the absorption at 620 nm and the potential of the bromide-selective electrode had reached stationary levels and Br_2MA had appeared, we bubbled argon into the reactor through a narrow hole in the Teflon stopper. Earlier bubbling can lead to escape of Br_2 along with the Ar bubbles and thus to incomplete bromination. After 5−10 min of bubbling, $Ru(bpy)_3^{2+}$ was added to the reactor. In some cases, a small quantity of bromide (10^{-4} M) was also added to the reactor in order to ensure that no BrO_3^- was left in the mixture. The addition of bromide does not affect the subsequent processes. Bubbling was continued for 5 more minutes, after which we started the illumination of the reaction mixture in the hermetically sealed reactor.

In separate experiment, we estimated the rate of decomposition of Br_2MA at $[H^+] = 0.5$ M by measuring the volume of CO_2 produced, V_{gas}. For $[Br_2MA] = 0.057$ M (prepared in reaction R10), we found that $dV_{gas}/dt = 0.07-0.08$ mL/min, which implies that the rate of Br_2MA decomposition is less than 1% per hour. At $[H^+] = 0.25$ M, the rate of decomposition is significantly smaller.

Figure 2a illustrates the method of our measurements. Curve (1) presents a typical experimental record of absorption at $\lambda =$ 620 nm (Abs-620). After the light is switched on, [Ru(III)] increases rapidly. We measure the initial rate of [Ru(III)] growth, $(d[Ru(III)]/dt)_0 \equiv V1$, as the initial slope of the kinetic curve (1). Later, Abs-620 reaches a stationary level, to which the steady-state concentration, $[Ru(III)]_{SS}$, corresponds. When the light is switched off, Abs-620 decreases exponentially to a final value that is always slightly higher than the starting level before illumination. We measure the initial rate of [Ru(III)] decrease, V3, as the slope of curve (1) immediately after switching the light off, and the first-order decay constant γ of this process in semilogarithmic coordinates $(\ln(A - A_\infty), t)$, where $A =$ Abs-620 and A_∞ is A as $t \rightarrow \infty$.

Curve (2) in Figure 2a shows the behavior of the potential U_{Br} of the bromide-selective electrode. The potential U_{Br} changes in a surprising fashion when the light is switched on and off. When the light is switched on, we observe a sharp *decrease* in $[Br^-]$ instead of the expected increase. On switching the light off, we see a rapid growth of $[Br^-]$, after which U_{Br} and, consequently, $[Br^-]$ reaches a stationary level. This behavior arises from the response of the bromide-selective electrode to Ru(III). A calibration curve for BrE in 0.5 M H_2SO_4 has the form $U_{Br} = a \log[Br^-] + b$, where $a \cong 57$ mV, $b \cong 120$ mV, and b depends on the type of reference electrode,

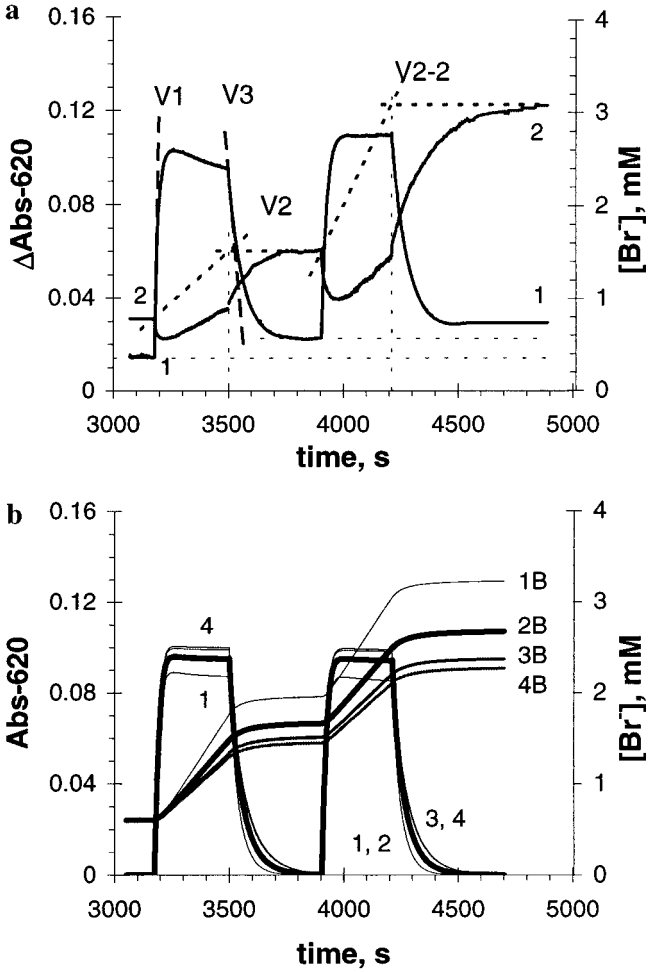

Figure 2. (a) Typical kinetic curves for experiments with Ru(II)−Br_2MA−H_2SO_4 subsystem. Two cycles of light on and off. Rapid growth and decrease in Abs-620 (curve 1) correspond to the moments of switching light on and off. To obtain Δ[Ru(III)] from changes in Abs-620 we used the relation ΔAbs-620 = Δ[Ru(III)]Δϵl, where Δϵ = 262 M^{-1} cm^{-1} and l = 3 cm. Curve 2 shows bromide-selective electrode potential recalculated for [Br^-] on the basis of calibration curve $U_{Br} = a \log[Br^-] + b$ obtained for solutions of bromide in sulfuric acid without Ru(III). Initial concentrations are $[H^+]_0$ = 0.5 M, [Ru(bpy)$_3^{2+}$]$_0$ = 1.5 × 10^{-4} M, [Br_2MA]$_0$ = 0.057 M. (b) Computer simulations for Ru(II)−Br_2MA−H_2SO_4 subsystem. All conditions as in Figure 2a. Curves 1B − 4B are [Br^-], curves 1−4 are Abs-620 (Abs-620 = [Ru(III)]lΔϵ_{620}), curves 3 and 4 coincide; for curves 1 and 1B k_{16} (M^{-1} s^{-1}) = 0.3 and k_{26} (M^{-1} s^{-1}) = 1 × 10^5, for curves 2 and 2B k_{16} = 0.2 and k_{26} = 2 × 10^5, for curves 3 and 3B k_{16} = 0.15 and k_{26} = 2 × 10^5, for curves 4 and 4B k_{16} = 0.15 and k_{26} = 1 × 10^5. All other constants as in Table 1.

the concentration of sulfuric acid, and the quality of the electrode surface. In the presence of Ru(III), b becomes significantly smaller, $b \cong$ 100 mV at [Ru(III)] = 1.5 × 10^{-4} M, while a does not change. The dependence of b on [Ru(III)] is monotonic, but not linear, and is probably associated with the electrode processes (adsorption − desorption of Ru(III) or reactions of Ru(III) with silver ions near the surface of the electrode membrane), which we did not study thoroughly. A decrease in b by Δb = 20 mV leads to an apparent decrease in [Br^-] by $10^{\Delta b/a}$, i.e., a factor of 2.2. Therefore, to assess the actual rate of [Br^-] growth during the period of illumination, d[Br^-]/d$t \equiv$ V2, we calculated the difference Δ[Br^-] between the stationary values of [Br^-] before and after illumination, when [Ru(III)] ≅ 0 (as shown in Figure 2a), and divided it by the time of illumination. The quantity of bromide producing during the dark

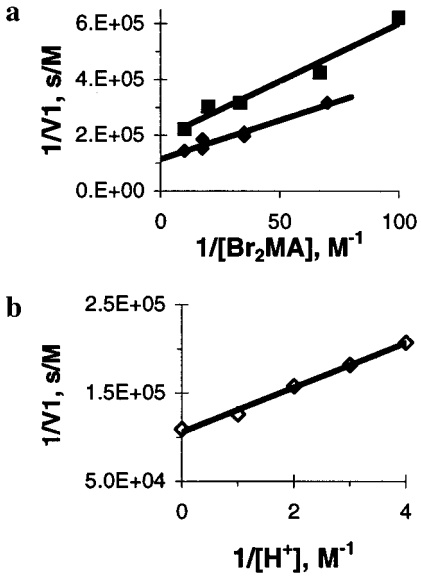

Figure 3. Dependence of 1/V1 on (a) 1/[Br_2MA] and (b) 1/[H^+]$_0$. Fixed initial conditions as in Figure 2. Value 1/V1 at 1/[H_2SO_4]$_0$ = 0 is obtained from data of Figure 3a and is equal to 1/$\upsilon(I_0)$.

stage of the process as a result of the reaction between Ru(III) and Br_2MA cannot exceed [Ru(II)]$_0$, or more precisely, [Ru(III)]$_{SS}$, which is much less (at least 10 times) than the total amount of bromide released during the illumination period and cannot significantly affect the calculated value V2. The electrode was calibrated each day in 0.5 M H_2SO_4, but sometimes this procedure was done after each experiment, as in the experiments with different concentrations of H_2SO_4.

Experiments with the subsystem MA−Br_2MA−Ru(II) were run in the same way as with the Br_2MA−Ru(II) subsystem, with the exception that after the bromination stage along with Ru(II) a small amount of malonic acid was added to the system. Experiments with the subsystem MA−BrMA−Br_2MA−Ru(II) were run as follows. The initial concentration of MA was fixed, while the sum [Br^-]$_0$ + [BrO_3^-]$_0 \equiv$ Br_0 varied among experiments, with the ratio [Br^-]$_0$/[BrO_3^-]$_0$ = 2 held constant. The final concentrations of BrMA and Br_2MA synthesized in the initial mixture of BrO_3^-, Br^-, MA, and H_2SO_4 were calculated by using the reaction scheme in Appendix 1. Experiments with the full BZ reaction but without BrMA were run as with the MA−Br_2MA−Ru(II) subsystem, except that after the bromination stage not only MA and Ru(II) but also BrO_3^- were added.

We obtained Ru(bpy)$_3^{3+}$ by oxidizing Ru(bpy)$_3^{2+}$ with an equimolar amount of Ce(IV).

III. Results

Br_2MA−Ru(bpy)$_3^{2+}$ Subsystem. The set of reactions R1, R2, and R9 gives for the rate V1

$$\left.\frac{\mathrm{d[Ru(III)]}}{\mathrm{d}t}\right|_{t=0} = \mathrm{V1} = \frac{\upsilon(I_0)k_9[\mathrm{Br_2MA}]}{k_2 + k_9[\mathrm{Br_2MA}]} \qquad (2)$$

The experimental dependence of 1/V1 on 1/[Br_2MA] for two different intensities of I_0 (with and without neutral density filters) is presented in Figure 3a, from which we find with the aid of eq 2 that k_2/k_9 = (2.2−2.4) × 10^{-2} M at [H^+] = 0.5 M and $\upsilon(I_0)$ = 8.8 × 10^{-6} M/s without ND filters. The value of $\upsilon(I_0)$ coincides surprisingly well with the value of $\upsilon(I_0)$ calculated with the aid of the power meter (see Appendix 2).

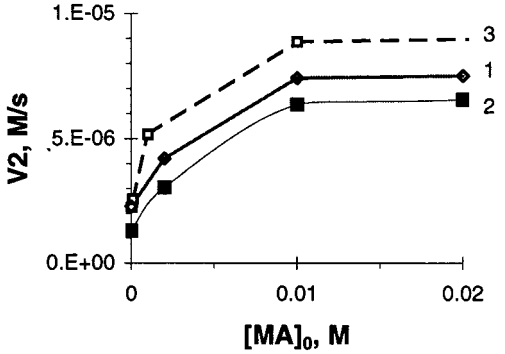

Figure 4. Dependence of bromide photo production rate V2 on $[MA]_0$ for organic subsystem MA−Br_2MA−Ru(II) at $[H^+]_0 = 0.5$ M, $[Ru(bpy)_3^{2+}]_0 = 1.5 \times 10^{-4}$ M, $[Br_2MA]_0$ (M) = (1) 0.057, (2) 0.0285 M, (3) 0.057 (simulations).

Reaction R9 may have, in general, different products, for example, Br_2 or Br^-,

$$Ru(II)^* + Br_2MA + H^+ \rightarrow Ru(III) + Br_2 + MA^\bullet \quad (R9a)$$

$$Ru(II)^* + Br_2MA \rightarrow Ru(III) + Br^- + BrMA^\bullet \quad (R9b)$$

If reaction R9a occurs, k_9 should depend on $[H^+]$, $k_9 = k_9'[H^+]$. In this case it follows from eq 2 that the dependence of 1/V1 on $1/[H^+]$ should be linear with slope $k_2/(v(I_0)k_9'[Br_2MA])$. The experimental dependence of 1/V1 on $1/[H^+]$ presented in Figure 3b substantiates this supposition. From the data in Figure 3b, we obtain $k_2/k_9' = 0.012$ M^2.

Organic Subsystem MA−Br_2MA−Ru(bpy)$_3^{2+}$. If reaction R9*a* occurs, the addition of a small amount of malonic acid to the Br_2MA−Ru(II) subsystem should markedly increase the rate of bromide photoproduction, V2, due to reaction R11,

$$Br_2 + CH_2(COOH)_2 \rightarrow CHBr(COOH)_2 + H^+ + Br^- \quad (R11)$$

the rate constant of which is equal to 29 M^{-1} s^{-1}, if $[Br_2] < 10^{-4}$ M.[17,18] Simultaneously, the addition of MA should slightly lower $[Ru(III)]_{SS}$ due to reaction R12,

$$Ru(III) + MA \rightarrow Ru(II) + MA^\bullet + H^+ \quad (R12)$$

The dependence of V2 on [MA] at different $[Br_2MA]_0$ is presented in Figure 4. V2 increases significantly up to $[MA]_0 = 0.01$ M, but then becomes nearly independent of $[MA]_0$.

In the course of a repeated light on−off cycle, the value of V2 in the MA−Br_2MA−Ru(II) subsystem does not change. For the Ru(II)−Br_2MA subsystem the same procedure leads to a noticeable increase in V2 (V2−2 in Figure 2a), while the rates V1 and V3 remain practically the same. These observations support the hypothesis that Br_2 is a product of reaction R9. At first there are no reactants that react with Br_2 in the Ru(II)−Br_2MA subsystem. Later, as organic products (for example, BrMA) are accumulated during illumination, Br_2 starts to react with them, producing Br^-.

Subsystem Br_2MA−Ru(II) with Hexane. To obtain direct evidence of Br_2 production in reaction R9 we performed experiments with the Br_2MA−Ru(II)−hexane subsystem, introducing a layer of hexane above the aqueous solution. If Br_2 is produced during illumination of the aqueous mixture, it should migrate into the hexane, where its solubility is considerably higher. The reaction was conducted in the same Teflon reactor filled with 5 mL of aqueous mixture and 10 mL of hexane with intense stirring of the aqueous phase. Hexane was added after the bromination. The level of the aqueous mixture was below the narrow windows through which the analyzing light enters and leaves the reactor, while the level of the oil phase was above the windows. Thus, only the absorption of the oil phase was measured. The wavelength of the analyzing light was 450 nm, which corresponds to the absorption band of Br_2, and the IF620 were replaced with interference filters of the appropriate wavelength. Actinic light entering the reactor through a large side window illuminated both the oil and the aqueous phases, which prevented us from measuring the $v(I_0)$ of reaction R1. A small quantity of bromine remaining in the aqueous mixture or in the vapor above the mixture after the bromination was responsible for the initial absorption of the oil phase before illumination.

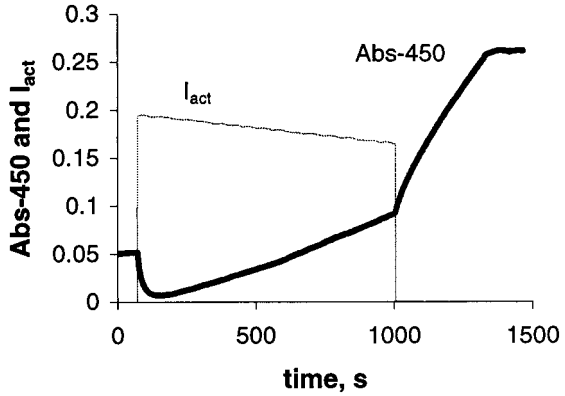

Figure 5. Kinetic curves for Abs-450 and I-460 (actinic light passed through the reactor) for experiments with Ru(II)−Br_2MA−H_2SO_4−hexane subsystem. Abs-450 is measured only in the oil phase.

After the actinic light is switched on, we observe a rapid decrease and then a slow increase in Abs-450 (Figure 5). After the light is switched off, Abs-450 grows considerably. These complex kinetics can be explained by two processes that affect Abs-450. First, Br^- is produced in the aqueous phase and may react with Br_2 in the oil phase through reactions R13.

$$Br_{2\,oil} \leftrightarrow Br_{2\,aq} \qquad Br_{2\,aq} + Br^-_{aq} \rightarrow Br_3^-{}_{aq} \quad (R13)$$

where the subscripts "oil" and "aq" refer to the oil and aqueous phases, respectively. Second, $[Br_2]_{oil}$ may be depleted by photodissociation of Br_2 via reaction R14

$$Br_2 + h\nu \rightarrow 2Br^\bullet \quad (R14)$$

which occurs in hydrocarbon solvents with a quantum yield approaching 1. Radicals $Br^\bullet$ produced in the oil phase may move to the aqueous phase. The reverse reaction R15 in the aqueous phase,

$$2Br^\bullet \rightarrow Br_2 \quad (15)$$

accompanied by diffusion of bromine molecules from the aqueous to the oil phase and slow stirring of the oil phase may account for the growth of $[Br_2]$ after the light is switched off. The spectrum of a sample taken from the oil phase is identical with the spectrum of Br_2 in hexane with $\lambda_{max} \cong 415$ nm.

Ru(II)−Br_2. We offer one further, indirect argument in support of reaction R9*a*. After the light is switched off in the Br_2MA−Ru(II) subsystem the concentration of Ru(III) decreases exponentially, but Abs-620 does not fall all the way to its initial level (see Figure 2a). Repeated cycles of switching the light on and off lead to further increases in the final value of Abs-620. The organic products do not absorb light at $\lambda = 620$ nm. We

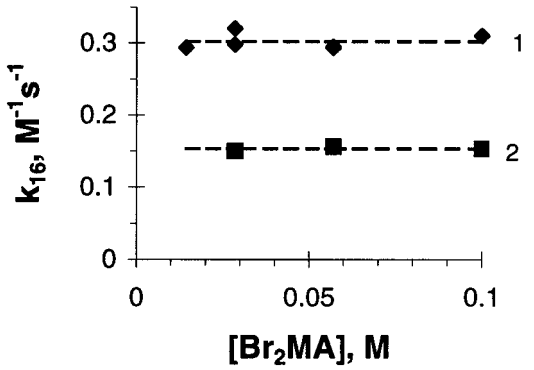

Figure 6. Dependence of rate constant k_{16} for reaction Br_2MA + Ru(III) on [Br_2MA]: curve 1, photooxidation of Ru(II) in subsystem Br_2MA−Ru(II); curve 2, Ru(III) generated via reaction of Ru(II) with Ce(IV).

suggest that this increase in Abs-620 is connected with the formation of an insoluble complex of Ru(II) with Br_2 (or with Br_3^-). This hypothesis is substantiated by an experiment in which we mix Ru(II) with a small amount of Br_2 (about 10^{-3}−10^{-2} M). This level of bromine should remain in the reactor after the first stage of bromination when the initial concentrations of Br^- and BrO_3^- were slightly higher than $4[MA]_0/3$ and $2[MA]_0/3$, respectively. In this experiment, a rust-colored sediment (precipitate) was formed and the solution became opaque. We conclude that Br_2 produced in reaction R9a leads to the formation of an insoluble complex with Ru(II), which is responsible for the observed increase in Abs-620. Note that in the dark reaction of Br_2MA with Ru(III), where the latter was obtained by adding Ce(IV) to a mixture of Ru(II) and Br_2MA, the value of Abs-620 returns to its initial level before adding Ce(IV).

Addition of malonic acid to the Br_2MA−Ru(II) subsystem after the cycle of switching the light on and off is completed and all values have reached stationary levels does not affect the final value of Abs-620. This observation confirms that an increase in the final value of Abs-620 is not connected either with the appearance of Br_2 in the solution or with any small amount of unreduced Ru(III). At the same time, addition of MA leads to further production of Br^-, which is especially noticeable at small concentrations of H_2SO_4 (at $[H_2SO_4] = 0.25$ M). Reaction R11 is the most plausible explanation for this process, which again implies that Br_2 is present in the solution. All these facts support our proposal of reaction R9a.

Dark Reactions of $Ru(bpy)_3^{3+}$. The kinetics of the system during the dark stage, after the light is switched off, are well described by expression 3,

$$[Ru(III)] = [Ru(III)]_{ss} \exp(-\gamma t) \qquad (3)$$

The Abs-620 decrease (exponential decay of [Ru(III)]) is probably associated with reaction R16,

$$Ru(III) + Br_2MA + H_2O \rightarrow Ru(II) + BrTA + H^+ + Br^\bullet \qquad k_{16} \quad (R16)$$

where BrTA is bromotartronic acid ($HOCBr(COOH)_2$). The exponent γ in eq 3 depends linearly on [Br_2MA], from which we calculate $k_{16} = \gamma/[Br_2MA] = 0.3\ M^{-1}\ s^{-1}$ (Figure 6, curve 1). This value may be an overestimate of k_{16}, since during illumination some bromoderivatives of malonic acid, e.g., BrMA, may be produced that react rapidly with Ru(III). Analysis of the dark reaction between Br_2MA and Ru(III), where the latter is obtained by oxidizing Ru(II) with Ce(IV), yields $k_{16} = 0.15\ M^{-1}\ s^{-1}$ (Figure 6, curve 2). These two values will be used later as upper and lower limits for k_{16} in our simulations.

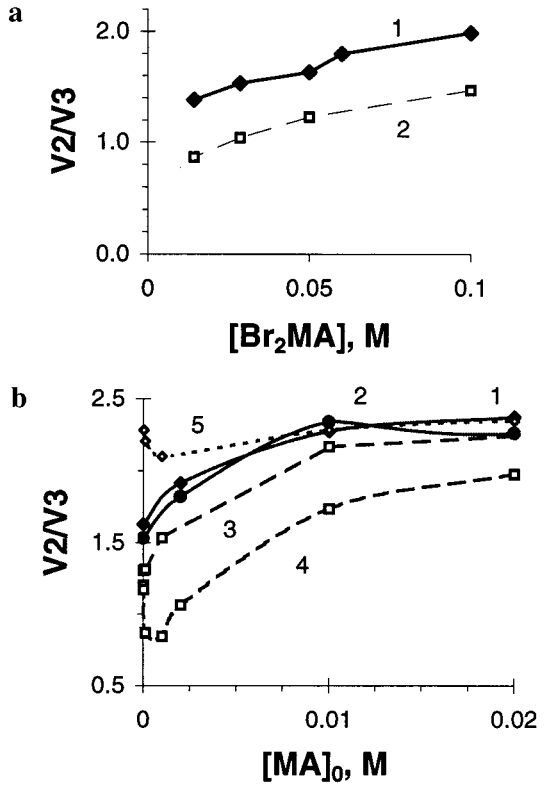

Figure 7. Dependence of n = V2/V3 (a) on [Br_2MA] for subsystem Br_2MA−Ru(II) (curve 1 is experiment, curve 2 is simulations) and (b) on [MA] for subsystem MA−Br_2MA−Ru(II) at $[H^+]_0 = 0.5$ M and $[Ru(bpy)_3^{2+}]_0 = 1.5 \times 10^{-4}$ M. Full curves 1 and 2 are experiment, dotted curves 3, 4, and 5 are results of simulations for models with reactions R9a, R9c, and R9b-H, respectively. $[Br_2MA]_0$ = (1, 3−5) 0.057 and (2) 0.0285 M.

We have also found that Ru(III) is reduced by bromide. This process may be written as

$$Ru(III) + Br^- \rightarrow Ru(II) + Br^\bullet \qquad k_{17} \quad (R17)$$

The reduction of Ru(III) in a large excess of bromide follows an exponential rate law, which gives $k_{17} = 0.17\ M^{-1}\ s^{-1}$.

Ratio V2/V3. The number of Br^- ions, n, released in the course of a single photooxidation−reduction cycle of a single catalyst molecule is given by the ratio of the bromide photoproduction rate (V2) to the rate of catalyst photooxidation, v_9, during the "stationary" illuminated portion of the cycle, $v_{9,SS}$. The rate $v_{9,SS}$ can easily be found from the condition that the process is stationary, from which it follows that the rates $v_{9,SS}$ and V3 are equal. Therefore, n = V2/V3. The dependence of V2/V3 on [Br_2MA] for the Br_2MA−Ru(II) subsystem is presented in Figure 7a. It is seen that n lies between 1.3 and 2.

The dependence of V2/V3 on [MA] for the MA−Br_2MA−Ru(II) subsystem is shown in Figure 7b. The number n increases with [MA] and approaches 2.5. A further increase in $[MA]_0$ (up to 0.2 M) results in only a slight growth of V2/V3.

On studying the dark reaction R16 at high concentrations of Ru(III) (10^{-3} to 4×10^{-3} M), we find that $\Delta[Br^-]/[Ru(III)]_0 = 1$, where $\Delta[Br^-]$ is the difference between the concentrations of bromide at the stationary levels before and after the reaction, which implies that reaction R16 leads to appearance of only a single bromide ion. The bromide ion is probably released in reaction R18

$$\mathrm{BrTA} \rightarrow \mathrm{MOA} + \mathrm{Br}^- + \mathrm{H}^+ \qquad k_{18} \qquad \text{(R18)}$$

where MOA is mesoxalic acid ($CO(COOH)_2$). Since $n \cong 2$, the remaining bromide ions are released in the Br_2MA-Ru and $MA-Br_2MA-Ru$ subsystems in reactions between Br_2 and various organic molecules.

Organic Subsystem MA−BrMA−Br$_2$MA−Ru(bpy)$_3^{2+}$. We now turn from overall reaction R10 to overall reaction R19,

$$3\mathrm{MA} + \mathrm{BrO_3}^- + 2\mathrm{Br}^- + 3\mathrm{H}^+ \rightarrow 3\mathrm{BrMA} + 3\mathrm{H_2O} \quad \text{(R19)}$$

which is the predominant stoichiometry at low values of $Br_0/[MA]_0$, where $Br_0 \equiv [BrO_3^-]_0 + [Br^-]_0$. Changes in the $[Br_2MA]/[BrMA]$ ratio allow us to assess the relative importance of reactions R6 and R9a for Br^- photoproduction.

Typical kinetic curves for $Br_0/[MA]_0 = 1.5$ and 1 are presented in Figure 8. We do not observe a major increase in [Ru(III)] when the light is switched on (curves 1 and 2). This observation is explained by the fact that the term k_7[Ru(III)][BrMA] in expression (4) for the rate d[Ru(III)]/dt, obtained from reactions R1, R2, R6, R7, R9a, R12, and R16, is relatively large, since BrMA is present at a significant level and k_7 is several hundred times larger than k_{12} and k_{16}.

$$\frac{\mathrm{d[Ru(III)]}}{\mathrm{d}t} = \frac{v(I_0)(k_6[\mathrm{Br_2MA}] + k_9[\mathrm{Br_2MA}])}{k_2 + k_6[\mathrm{Br_2MA}] + k_9[\mathrm{Br_2MA}]} - [\mathrm{Ru(III)}](k_{12}[\mathrm{MA}] + k_7[\mathrm{BrMA}] + k_{16}[\mathrm{Br_2MA}]) \quad (4)$$

We were able to measure V1 and V3 reliably only when $Br_0/[MA]_0 \geq 1.5$. Figure 8 shows that Abs-620 grows in the course of illumination, which we attribute to formation of the insoluble complex $Ru(II)-Br_2$. The behavior of the bromide-selective electrode (curves 3 and 4) at high values of [BrMA] (when $Br_0/[MA]_0 < 1.5$) accords with our expectations, because the concentration of Ru(III) affecting the electrode response is very low.

We show in Figure 9 how V2, V2/V3, [BrMA] and $[Br_2MA]$ depend on Br_0. As Br_0 decreases, [BrMA] rises, but V2 decreases except in a narrow region near $Br_0 = 0.2$ M (Figure 9c). We conclude that Br_2MA plays a determining role in the Br^- photoproduction rate when $Br_0/[MA]_0 > 0.5$. The increase in n = V2/V3 as Br_0 decreases is explained by the reactions of Br_2 with MA and BrMA. The fact that n approaches 3 at $Br_0 = 0.15$ suggests that radical reactions of the bromo-derivatives of malonic acid may play a significant role as well.

Full BZ Reaction. By employing the complete bromination of malonic acid (reaction R10), we may construct a photosensitive BZ oscillator without BrMA. The behavior of such an oscillator is illustrated in Figure 10. This oscillator operates near the fully oxidized state of the catalyst. Switching the light on leads to significant production of Br^- and to the suppression of oscillations.

Figure 11 shows a BZ system with initial reagents BrO_3^-, MA, and Ru(II) only, without BrMA and Br_2MA. All concentrations are the same as in the experiment shown in Figure 10, except that $[MA]_{11} = [MA]_{10} + [Br_2MA]_{10}$ (subscripts "11" and "10" refer to concentrations in Figures 11 and 10, respectively). The data in Figures 10 and 11 show the difference in photo response of the BZ reaction with and without Br_2MA at the same light intensity. Without Br_2MA, the light fails to suppress oscillations. Moreover, we observe an opposite action of light related to the photoproduction of $BrO_2^\bullet$ (reaction R3). Switching the light on accelerates the autocatalytic stage and leads to an earlier start of Ru(III) growth than expected from the dark oscillations (Figure 11b) as well as to an increase in the minimum of [Ru(III)] (Figure 11a). Switching the light off,

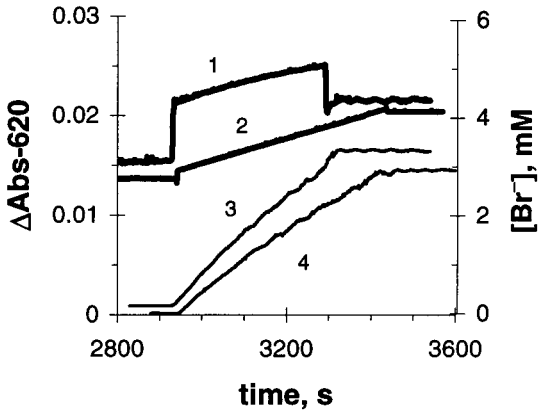

Figure 8. Kinetic curves for experiments with Ru(II)−MA−BrMA−$Br_2MA-H_2SO_4$ subsystem. One cycle of light on and off. Sharp changes in derivative dAbs-620/dt correspond to moments of switching light on and off. Initial concentrations are $[H^+]_0 = 0.5$ M, $[MA]_0 = 0.1$ M, $[Ru(bpy)_3^{2+}]_0 = 1.5 \times 10^{-4}$ M, Br_0 (M) = (1, 3) 0.15, (2, 4) 0,1. Curves (1) and (2) are Abs-620, curves (3) and (4) are $[Br^-]$.

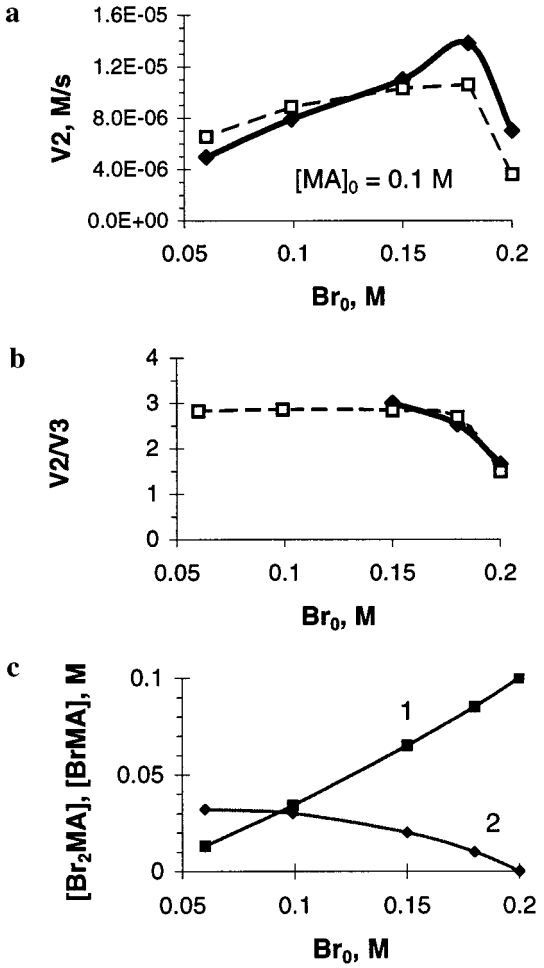

Figure 9. Dependence of bromide photo production rate V2 (a) and V2/V3 (b) on $Br_0 = [Br^-]_0 + [BrO_3^-]_0$ for organic subsystem MA−BrMA−Br_2MA−Ru(II) at $[H_2SO_4]_0 = 0.5$ M, $[Ru(bpy)_3^{2+}]_0 = 1.5 \times 10^{-4}$ M, [MA] + [BrMA] + $[Br_2MA] = 0.1$ M. White squares with dotted line are results of computer simulations using the reaction scheme in Table 1. (c) Dependence of final concentrations of (1) Br_2MA and (2) BrMA on Br_0 in a MA − Br^- − BrO_3^- − H_2SO_4 mixture calculated using the reaction scheme in Appendix 1. These concentrations are used as the initial concentrations in simulations of the reaction scheme in Table 1.

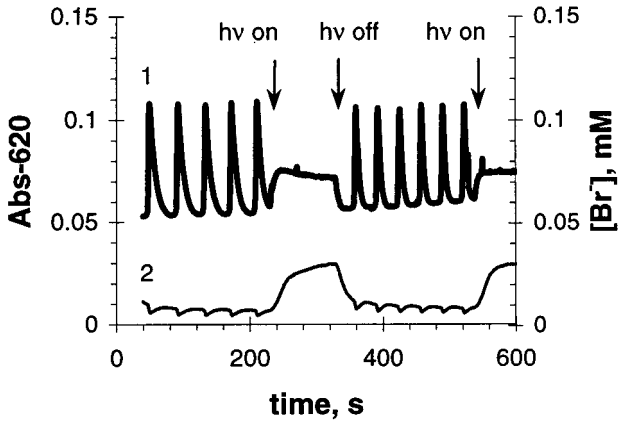

Figure 10. Photosensitive oscillations in Ru(bpy)$_3^{2+}$-catalyzed BZ reaction with MA and Br_2MA. Conditions: $[H_2SO_4]_0 = 0.5$ M, [Ru(bpy)$_3^{2+}$]$_0 = 1 \times 10^{-4}$ M, $[BrO_3^-]_0 = 0.075$ M, $[MA]_0 = 0.05$ M, $[Br_2MA]_0 = 0.1$ M. Curve 1 is Abs-620; curve 2 is $[Br^-]$.

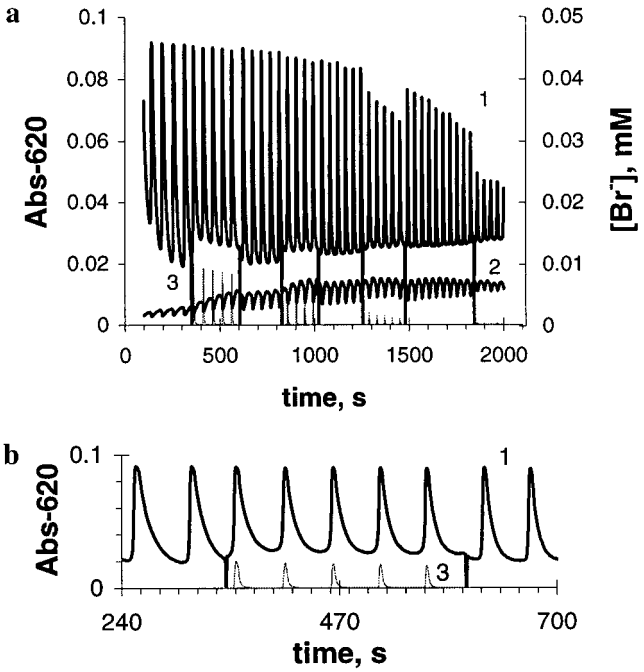

Figure 11. Photosensitive oscillations in Ru(bpy)$_3^{2+}$-catalyzed BZ reaction with MA. (1) Abs-620, (2) $[Br^-]$, and (3) intensity of actinic light at $\lambda = 460$ nm in relative units. Conditions: $[H_2SO_4]_0 = 0.5$ M, [Ru(bpy)$_3^{2+}$]$_0 = 1 \times 10^{-4}$ M, $[BrO_3^-]_0 = 0.075$ M, $[MA]_0 = 0.15$ M. (b) is enlarged fragment of full record (a). Vertical lines drawn between curve 1 and time axis correspond to moments of switching light on and off.

on the other hand, delays the autocatalytic stage (Figure 11b). Later in the reaction, BrMA builds up in the system, and the system becomes more sensitive to light (see Figure 11a at $t >$ 1200 s). Now the action of light causes a decrease in the maximum of [Ru(III)] as a result of the inhibition of the autocatalytic stage.

IV. Simulations and Discussion

Since all the rate constants of the reactions with Ru(II), Ru(II)*, and Ru(III) are measured in this work or known from the literature, simulation of the behavior of Ru(III) (Abs-620-(t)) is straightforward. Simulating the bromide kinetics and the dependence of V2/V3 on [MA] or on $[Br_2MA]$ is more difficult, since the rate of Br^- production depends to a great extent on reactions involving MA$^\bullet$, BrMA$^\bullet$, and Br$^\bullet$ radicals, whose rate constants are not as accurately known.

To simulate the photoresponse of all three subsystems studied in this work, we used a model composed of reactions R1, R2, R6−R9a, R11, R12, R15−R18 supplemented with the radical reactions R20−R34 as well as with bromine hydrolysis, R35−R36. All reactions used and their rate constants are given in Table 1. The rate of reaction R1 depends on the light intensity I_0 and [Ru(II)]. The exact dependence of $v(I_0)$ on I_0 and [Ru(II)], calculated in Appendix 2, eq A2-2, is rather cumbersome and poorly suited to numerical simulations. Therefore, we used the approximation of expression A2-2 by expression A2-3.

First, we study the sensitivity of the rate of bromide photoproduction (V2) to the rate constants k_{16} and k_{26}. The results of our simulations for the [Ru(III)] (in the form of [Ru(III)]$l\Delta\epsilon_{620}$ = Abs-620) and $[Br^-]$ kinetics for different values of k_{16} and k_{26} are presented in Figure 2b. All initial concentrations and times of switching the light on and off are the same as in Figure 2a. Comparison of Figure 2a,b shows that the experimental and calculated curves agree rather well, given that our model neglects the formation of the insoluble complex Ru(II)−Br_2. The values $k_{16} = 0.2$ M^{-1} s^{-1} and $k_{26} = 2 \times 10^5$ M^{-1} s^{-1} give the best fit.

Next, we vary the other rate constants of radical reactions and examine the response of V2. We find that V2 is practically insensitive to severalfold changes in k_{15}, k_{20}, k_{23}, k_{24}, k_{27}, k_{28}, and $k_{30} - k_{34}$, while V2 is quite sensitive to the values of k_{21}, k_{22}, k_{25}, and k_{29}. The simulations show that for the Br_2MA−Ru(II) subsystem under illumination $[Br_2]$ and [BrMA] first increase and then reach approximately the same stationary level. For our experimental conditions, $[Br_2]_{SS}$ ranges from 6×10^{-5} to 1.6×10^{-4} M and $[BrMA]_{SS}$ from 10^{-4} to 2×10^{-4} M, with the higher values obtained for larger $[Br_2MA]_0$. In the MA−Br_2MA−Ru(II) subsystem, $[Br_2]_{SS}$ is several times smaller than the corresponding value of $[Br_2]_{SS}$ in the Br_2MA−Ru(II) subsystem, and [BrMA] does not reach a stationary level during the period of illumination (300−500 s) but grows monotonically with time. The rate of [BrMA] accumulation is slightly smaller (50−10% for $[MA]_0 = 0.01-0.1$ M) than the rate of bromide ion production, because at high [MA] reaction R16 becomes ineffective due to competition with reaction R12, and the main channel for bromide ion production is the subsequent reactions R9a and R11. The calculated dependences of V2 and V2/V3 on Br_2MA, MA, and Br_0 are also quite close to the experimental results (see Figures 4, 7, and 9).

Since reaction R25 converts the products of reaction R9a from Br_2 and MA$^\bullet$ into Br$^\bullet$ and BrMA, we might suppose that reaction R9 proceeds as follows:

$$\text{Ru(II)}^* + \text{Br}_2\text{MA} + \text{H}^+ \rightarrow \text{Ru(III)} + \text{Br}^\bullet + \text{BrMA} \quad \text{(R9c)}$$

In this case Br_2 would still be produced (for example, via reaction R15), but its steady state concentration would be significantly smaller. We have simulated this case by replacing reaction R9a with R9c. The resulting dependence of V2/V3 on $[MA]_0$ (Figure 7b, curve 4) for the MA−Br_2MA−Ru(II) subsystem is notably different from the experimental one and, consequently, we reject reaction R9*c*.

Yamaguchi et al.[15] showed that the rate of reaction R6 depends linearly on $[H^+]$ and reaction R6 should be written as[14]

$$\text{Ru(II)}^* + \text{BrMA} + \text{H}^+ \rightarrow \text{Ru(III)} + \text{Br}^- + \text{products} \quad \text{(R6-H)}$$

By analogy with R6-H, reaction R9b may also be dependent

TABLE 1: Reactions Included in the Model for Photoresponse of Organic Subsystems of the BZ Reaction and Their Rate Constants

	reaction	constant	ref
R1	$Ru(II) + h\nu \rightarrow Ru(II)^*$	$v_{max} = 8.8 \times 10^{-6}$ M/s $K_1 = 4 \times 10^{-5}$ M	this work[a]
R2	$Ru(II)^* \rightarrow Ru(II)$	1.7×10^6 s^{-1}	25, 26*b*
R6	$Ru(II)^* + BrMA \rightarrow Ru(III) + MA^\bullet + Br^-$	1.9×10^7 M^{-1} s^{-1}	16
R9a	$Ru(II)^* + Br_2MA + H^+ \rightarrow Ru(III) + Br_2 + MA^\bullet$	1.48×10^8 M^{-2} s^{-1}	this work
R12	$Ru(III) + MA \rightarrow Ru(II) + MA^\bullet + H^+$	0.2 M^{-1} s^{-1}	27
R7	$Ru(III) + BrMA \rightarrow Ru(II) + BrMA^\bullet + H^+$	55 M^{-1} s^{-1}	27
R16	$Ru(III) + Br_2MA + H_2O \rightarrow Ru(II) + Br^\bullet + H^+ + BrTA$	0.2 M^{-1} s^{-1}	this work
R17	$Ru(III) + Br^- \rightarrow Ru(II) + Br^\bullet$	0.17 M^{-1} s^{-1}	this work
R18	$BrTA \rightarrow MOA + Br^- + H^+$	1 s^{-1}	17
R15	$2Br^\bullet \rightarrow Br_2$	1×10^8 M^{-1} s^{-1}	28
R11	$Br_2 + MA \rightarrow BrMA + H^+ + Br^-$	29 M^{-1} s^{-1}	17, 18
R8	$Br_2 + BrMA \rightarrow Br_2MA + H^+ + Br^-$	53 M^{-1} s^{-1}	18
R20	$Br^\bullet + MA^\bullet \rightarrow BrMA$	1×10^9 M^{-1} s^{-1}	28
R21	$Br^\bullet + BrMA^\bullet \rightarrow Br_2MA$	3×10^9 M^{-1} s^{-1}	28
R22	$2BrMA^\bullet + H_2O \rightarrow BrMA + BrTA$	5×10^7 M^{-1} s^{-1}	28
R23	$2MA^\bullet + H_2O \rightarrow MA + TA$	4.2×10^8 M^{-1} s^{-1}	29, 30
R24	$MA^\bullet + BrMA^\bullet + H_2O \rightarrow MA + BrTA$	1×10^9 M^{-1} s^{-1}	28
R25	$MA^\bullet + Br_2 \rightarrow BrMA + Br^\bullet$	1.5×10^8 M^{-1} s^{-1}	28, 31
R26	$MA^\bullet + Br_2MA \rightarrow BrMA + BrMA^\bullet$	2×10^5 M^{-1} s^{-1}	this work[c]
R27	$MA^\bullet + BrMA \rightarrow MA + BrMA^\bullet$	1×10^5 M^{-1} s^{-1}	28
R28	$Br^\bullet + MA \rightarrow Br^- + MA^\bullet + H^+$	2×10^5 M^{-1} s^{-1}	28
R29	$Br^\bullet + BrMA \rightarrow Br^- + BrMA^\bullet + H^+$	1×10^5 M^{-1} s^{-1}	this work
R30	$Br^\bullet + MOA + H_2O \rightarrow Br^- + OA + {}^\bullet COOH + H^+$	2×10^3 M^{-1} s^{-1}	28
R31	$Br^\bullet + {}^\bullet COOH \rightarrow Br^- + CO_2 + H^+$	1×10^9 M^{-1} s^{-1}	28
R32	$Br^\bullet + OA \rightarrow Br^- + {}^\bullet COOH + CO_2 + H^+$	2×10^3 M^{-1} s^{-1}	28
R33	$Ru(III) + {}^\bullet COOH \rightarrow Ru(II) + CO_2 + H^+$	1×10^8 M^{-1} s^{-1}	this work
R34	${}^\bullet COOH + {}^\bullet COOH \rightarrow OA$	1×10^9 M^{-1} s^{-1}	28
R35	$Br_2 \rightarrow HOBr + Br^- + H^+$	80 s^{-1}	27
R36	$HOBr + Br^- + H^+ \rightarrow Br_2$	8×10^9 M^{-2} s^{-1}	27

[a] Rate of reaction R1 is expressed as $v(I_0) = v_{max}[Ru(II)]/(K_1 + [Ru(II)])$; see Appendix 2. [b] Rate of reaction R2 is known for aqueous solution at pH = 7.0. Since only the ratios k_6/k_2 and k_9/k_2 are important for our simulations, we used $k_2 = 1.7 \times 10^6$ s^{-1} as a reference value and calculated the values of k_6 and k_9 from these ratios. [c] We assume that k_{26} is the same order of magnitude as the rate constant for reaction R27.[28] MOA is mesoxalic acid ($CO(COOH)_2$), OA is oxalic acid ($(COOH)_2$), and TA is tartronic acid ($CHOH(COOH)_2$).

on $[H^+]$. In this case, R9b could be rewritten as

$$Ru(II)^* + Br_2MA + H^+ \rightarrow Ru(III) + Br^- + BrMA^\bullet + H^+ \quad \text{(R9b-H)}$$

We have also simulated this case, replacing reaction R9a by R9b-H and have found that V2/V3 is then nearly independent of $[MA]_0$ in the MA−Br_2MA−Ru(II) subsystem, and V2/V3 = 2.3−2.1 at $[MA]_0$ = 0−0.02 M (see curve 5 in Figure 7b). For this reason, we also reject reaction R9b-H.

Recent HPLC results[21,22] suggest that the products of reactions R22 and R23 differ from those in Table 1, and that these reactions should be rewritten as

$$2BrMA^\bullet \rightarrow CO_2 + Br^- + H^+ + (COOH)_2C{=}CBrCOOH \quad \text{(R22a)}$$

$$2MA^\bullet \rightarrow (HOOC)_2CHCH(COOH)_2 \quad \text{(R23a)}$$

In addition, EPR experiments[23] imply that reaction R27 can be neglected. Our simulations indicate that the dependence of V2 and V3 on the initial reagent concentrations is nearly insensitive to the rate constants k_{23} and k_{27}. Therefore, neither the identity of the products of reaction R23 or the neglect of reaction R27 has a significant effect on our simulations. To test whether the products of reaction R22 are important, we replaced reaction R22 by R22a with the same rate constant k_{22}. We found no changes in the results. Indeed, the rate of bromide production remains unchanged, because one of the products of reaction R22, BrTA, quickly decomposes in reaction R18 to produce Br^-, which is generated directly in reaction R22a. Only the rate of BrMA production may be affected by replacing R22 by R22a, but the major contribution to the rate of BrMA production is made by reaction R25 at low [MA] and R26 or R11 at high [MA].

Since the model considered is in good accord with the experimental data, we have neglected possible effects on Br^- release of other reactions, such as the hydrolysis of $BrMA^\bullet$ and reactions of Br_2MA with $BrMA^\bullet$ and $Br^\bullet$, as well as the photodecomposition of Br_2 into $2Br^\bullet$.

V. Conclusion

We have discovered and characterized a new photosensitive stage in the BZ reaction catalyzed by $Ru(bpy)_2^{2+}$. At the H_2SO_4 concentrations typically used in experiments on the BZ system, dibromomalonic acid reacts with Ru(II)* faster than bromomalonic acid and produces more bromide ions per photon at sufficiently high concentrations of malonic acid.

Reaction R9a may play a major role in experiments on the photocontrol of patterns in spatially extended BZ systems.

Acknowledgment. V.K.V. thanks Lingfa Yang and Milos Dolnik for supplying us with software for solving ordinary differential equations. This work was supported by the Chemistry Division of the National Science Foundation and the W. M. Keck Foundation.

Appendix 1. Reaction Scheme for the Bromination of Malonic Acid in the Mixture of MA−Br^-−BrO_3^-−H_2SO_4[18]

In the reactions below, MA is the keto form of malonic acid, MA_E is the enol form of malonic acid, BrMA is the keto form

of bromomalonic acid, and $BrMA_E$ is the enol form of bromomalonic acid.

A1-1 $BrO_3^- + Br^- + 2H^+ \rightarrow HBrO_2 + HOBr$ $k_1 = 1.6\ M^{-3}\ s^{-1}$

A1-2 $HBrO_2 + Br^- + H^+ \rightarrow 2HOBr$ $k_2 = 2.5 \times 10^6\ M^{-2}\ s^{-1}$

A1-3 $2HBrO_2 \rightarrow HOBr + BrO_3^- + H^+$ $k_3 = 3 \times 10^3\ M^{-1}\ s^{-1}$

A1-4 $HOBr + HBrO_2 \rightarrow Br^- + BrO_3^- + 2H^+$ $k_4 = 3.2\ M^{-1}\ s^{-1}$

A1-5 $HOBr + Br^- + H^+ \rightarrow Br_2 + H_2O$ $k_5 = 8 \times 10^9\ M^{-2}\ s^{-1}$

A1-6 $Br_2 + H_2O \rightarrow HOBr + Br^- + H^+$ $k_6 = 80\ s^{-1}$

A1-7 $MA \rightarrow MA_E$ $k_7 = 2.6 \times 10^{-3}\ s^{-1}$

A1-8 $MA_E \rightarrow MA$ $k_8 = 180\ s^{-1}$

A1-9 $Br_2 + MA_E \rightarrow BrMA + Br^- + H^+$ $k_9 = 2.0 \times 10^6\ M^{-1}\ s^{-1}$

A1-10 $HOBr + MA_E \rightarrow BrMA + H_2O$ $k_{10} = 0.67 \times 10^6\ M^{-1}\ s^{-1}$

A1-11 $BrMA \rightarrow BrMA_E$ $k_{11} = 1.2 \times 10^{-2}\ s^{-1}$

A1-12 $BrMA_E \rightarrow BrMA$ $k_{12} = 0.8 \times 10^3\ s^{-1}$

A1-13 $Br_2 + BrMA_E \rightarrow Br_2MA + Br^- + H^+$ $k_{13} = 3.5 \times 10^6\ M^{-1}\ s^{-1}$

A1-14 $HOBr + BrMA_E \rightarrow Br_2MA + H_2O$ $k_{14} = 1.1 \times 10^6\ M^{-1}\ s^{-1}$

Appendix 2. Direct Calculation of the Rate of Reaction R1, $v(I_0)$

The power P of the incident light may be calculated from formula (A2-1):

$$P_{th} = \theta S \int_\lambda T(\lambda)\, I_0(\lambda)\, d\lambda \qquad \text{(A2-1)}$$

where $I_0(\lambda)$ is the spectrum of the lamp used, $T(\lambda)$ is the transmission spectrum of the filters through which light passes (filter F2); θ is the fraction of the total light emitted by the lamp that enters the reactor's window; S is the cross-sectional area of the incident light beam (S is smaller than the reactor's window area). For our 150 W xenon lamp (Oriel), $I_0(\lambda) = 1.8-2$ $\mu W\ cm^{-2}\ nm^{-1}$ at 50 cm distance in the range between 400 and 500 nm.[24] Comparison of P_{th} calculated by formula A2-1 with the measured value of P_{exp} (in our case, P_{exp} measured by the power meter is 20 mW)) gives us the product θS.

The rate of reaction R1, $v(I_0)$, in M/s can be written as[20]

$$v(I_0) = \frac{P_{exp}}{P_{th}} \frac{1}{VN_A} \int_\lambda T(\lambda) \frac{I_0(\lambda)}{h\nu} \frac{1 - 10^{-A(\lambda)}}{A(\lambda)} \epsilon(\lambda)[\text{Ru(II)}]l\, d\lambda \qquad \text{(A2-2)}$$

where V is the volume of the mixture in the reactor ($V = 20$ mL), l is the optical path length of the incident light beam, $I_0(\lambda)/h\nu$ is the number of photons of wavelength λ passing through a 1 cm^2 square per second, h is Planck's constant, $\nu = c/\lambda$, c is the velocity of light, $\epsilon(\lambda)$ is the extinction coefficient of the photosensitive molecule, Ru(II) in our case, and $A(\lambda)$ is the spectrum of the illuminated solution in units of optical density. All values in formula A2-2 are known and $v(I_0)$ can be calculated exactly. A simple approximation for eq A2-2 in our case is as follows:

$$v(I_0) = v_{max}[\text{Ru(II)}]/(K_1 + [\text{Ru(II)}]) \qquad \text{(A2-3)}$$

where $v_{max} = 0.9 \times 10^{-5}$ M/s (depending on the filter F2 used) and $K_1 \cong 4 \times 10^{-5}$ M. The constant K_1 was obtained by the method of least squares. The value v_{max} is equal to P_{exp} measured in moles of photons entering a volume $V = 20$ mL per second.

References and Notes

(1) Kuhnert, L.; Agladze, K. I.; Krinsky, V. I. *Nature* **1989**, *337*, 244.
(2) Petrov, V.; Ouyang, Qi.; Swinney, H. L. *Nature* **1997**, *388*, 655.
(3) Ram Reddy, M. K.; Nagy-Ungvarai, Zs.; Müller, S. C. *J. Chem. Phys.* **1994**, *98*, 12255.
(4) Petrov, V.; Ouyang, Qi.; Li, G.; Swinney, H. L. *J. Phys. Chem.* **1996**, *100*, 18992.
(5) Zykov, V. S.; Mikhailov, A. S.; Müller, S. C. *Phys. Rev. Lett.* **1997**, *78*, 3398.
(6) Amemiya, T.; Kettunen, P.; Kádár, S.; Yamaguchi, T.; Showalter, K. *Chaos* **1998**, *8*, 872.
(7) Amemiya, T.; Ohmori, T.; Nakaiwa, M.; Yamaguchi, T. *J. Phys. Chem. A* **1998**, *102*, 4537.
(8) Kádár, S.; Wang, J.; Showalter, K. *Nature* **1998**, *391*, 770.
(9) Amemiya, T.; Ohmori, T.; Yamamoto, T.; Yamaguchi, T. *J. Phys. Chem. A* **1999**, *103*, 3451.
(10) Kaminaga, A.; Hanazaki, I. *J. Phys. Chem. A* **1998**, *102*, 3307.
(11) Mori, Y.; Nakamichi, Y.; Sekiguchi, T.; Okazaki, N.; Matsumura, T.; Hanazaki, I. *Chem. Phys. Lett.* **1993**, *211*, 421.
(12) Ram Reddy, M. K.; Slávik, Z.; Nagy-Ungvarai, Zs.; Müller, S. C. *J. Phys. Chem.* **1995**, *99*, 15081.
(13) Srivastava, P. K.; Mori, Y.; Hanazaki, I. *Chem. Phys. Lett.* **1992**, *190*, 279.
(14) Amemiya, T.; Ohmori, T.; Yamaguchi, T. *J. Phys. Chem. A* **2000**, *104*, 336.
(15) Yamaguchi, T.; Shimamoto, Y.; Amemiya, T.; Yoshimoto, M.; Ohmori, T.; Nakaiwa, M.; Akiya, T.; Sato, M.; Matsumura-Inoue, T. *Chem. Phys. Lett.* **1996**, *259*, 219.
(16) Kadar, S.; Amemiya, T.; Showalter, K. *J. Phys. Chem. A* **1997**, *101*, 8200.
(17) Försterling, H.-D.; Stuk, L.; Barr, A.; McCormic, W. D. *J. Phys. Chem.* **1993**, *97*, 2623.
(18) Sirimungkala, A.; Försterling, H.-D.; Dlask, V.; Field, R. J. *J. Phys. Chem. A* **1999**, *103*, 1038.
(19) Grill, S.; Zykov, V. S.; Müller, S. C. *Phys. Rev. Lett.* **995**, *75*, 3368.
(20) Vanag, V. K.; Alfimov, M. V. *J. Phys. Chem.* **1993**, *97*, 1878.
(21) Oslonovitch, J.; Försterling, H.-D.; Wittmann, M.; Noszticzius, Z. *J. Phys. Chem. A* **1998**, *102*, 922.
(22) Sirimungkala, A.; Försterling, H.-D.; Noszticzius, Z. *J. Phys. Chem.* **1996**, *100*, 3051.
(23) Försterling, H.-D.; Stuk, L. *J. Phys. Chem.* **1991**, *95*, 7320.
(24) Drozdowicz, Z. *Catalog. The Book of Photon Tools*; Oriel Instruments: Stratford, CT, 1999.
(25) Mulazzani, Q. G.; Sun, H.; Hoffman, M. Z.; Ford, W. E.; Rodgers, M. A. J. *J. Phys. Chem.* **1994**, *98*, 1145.
(26) Park, J. W.; Kim, M.-H.; Ko, S. H.; Paik, Y. H. *J. Chem. Phys.* **1993**, *97*, 5424.
(27) Gao, Y.; Försterling, H.-D. *J. Phys. Chem.* **1995**, *99*, 8638.
(28) Györgyi, L.; Turányi, T.; Field, R. J. *J. Phys. Chem.* **1990**, *94*, 7162.
(29) Brusa, M. A.; Perissinotti, L. J.; Colussi, A. *J. Phys. Chem.* **1985**, *89*, 1572.
(30) Försterling, H.-D.; Stuk, L. *J. Phys. Chem.* **1992**, *96*, 3067.
(31) Försterling, H.-D.; Noszticzius, Z. *J. Phys. Chem.* **1989**, *93*, 2740.